

# Better Foreground Segmentation Through Graph Cuts

Nicholas R. Howe

Alexandra Deschamps

Computer Science  
Smith College  
Northampton, MA 01063

## Abstract

*For many tracking and surveillance applications, background subtraction provides an effective means of segmenting objects moving in front of a static background. Researchers have traditionally used combinations of morphological operations to remove the noise inherent in the background-subtracted result. Such techniques can effectively isolate foreground objects, but tend to lose fidelity around the borders of the segmentation, especially for noisy input. This paper explores the use of a minimum graph cut algorithm to segment the foreground, resulting in qualitatively and quantitatively cleaner segmentations. Experiments on both artificial and real data show that the graph-based method reduces the error around segmented foreground objects. A MATLAB code implementation is available at <http://www.cs.smith.edu/~nhowe/research/code/#fgseg>.*

## 1. Introduction

Many computer vision applications require the segmentation of foreground from background as a prelude to further processing. Although difficult in the general case, the task can be greatly simplified if the object or objects of interest in the foreground move across a static background. Such situations arise or can be engineered in a wide variety of applications, including security videos, video-based tracking and motion capture, sports ergonomics, and human-computer interactions via inexpensive workstation-mounted cameras.

All of these applications rely on or would benefit from high-quality foreground segmentation. Unfortunately, existing methods sometimes prove unreliable and error-prone. Furthermore, the results can vary greatly between successive frames of a video. This paper introduces a new way to compute the foreground segmentation that makes fewer errors and can be temporally stabilized from frame to frame.

Traditionally, researchers solve the foreground segmentation problem with static background through a procedure called *background subtraction*. In this approach, the com-

puter builds a model of the static background, either off-line or updated dynamically after each frame in the video stream, and then compares the next frame with the background model on a per-pixel basis. Pixels that differ sufficiently from the background model may be deemed part of the foreground, at least in the ideal case. If the calculation were free of noise, one could simply fix a threshold and declare anything sufficiently different from the background to be part of the foreground.

Unfortunately, a number of confounding factors make perfect background subtraction unattainable. Camera noise (particularly in inexpensive CCD cameras) ensures that even background pixels will not exhibit constant values from frame to frame, but will instead show a distribution around some characteristic value. If the background contains non-static elements (such as vegetation, cloth, or gravel) then the variance in the measurements of background pixels may be quite large. Moving objects in the foreground may cause shadows and reflections to fall on background areas, changing their appearance significantly. The foreground objects may lack sufficient contrast with the background areas they obscure, either through deliberate camouflage or by chance. In consequence, comparison of a pixel in a given frame with the background model for that pixel cannot definitively classify the pixel as either foreground or background without some potential for error.

Errors at a single pixel may be mitigated by aggregating the results over some local neighborhood of pixels. Researchers have traditionally taken this approach to cleaning up the errors in the thresholded image. A combination of morphological operations on the binary thresholded image removes isolated foreground and background pixels, generating a better approximation to the silhouettes of the moving objects in the foreground. Unfortunately, the same approach can obliterate details at the edges of the silhouette.

This work departs from the standard practice by using an algorithm based upon the minimum graph cut to separate the foreground from the background. The algorithm presented herein uses information that would be thrown away by thresholding to construct a graph incor-

porating all the differences measured between the current frame and the background model. Links in this graph reflect the connectivity of the pixels in the image, allowing each pixel to affect those in its local neighborhood. (Details of the graph construction appear below.) Segmenting the graph using a standard graph-cut algorithm produces a foreground-background segmentation that can correct local errors without introducing larger global distortions. Qualitatively, the results using the new technique look cleaner and more correct; the quantitative tests in Section 4.1 show that the method produces fewer errors than do current practices when compared to human-segmented ground truth.

The remainder of this paper conducts an in-depth look at the old and new methods for foreground segmentation using background subtraction. Section 2 describes the two algorithms that Sections 3 and 4 compare experimentally. Section 5 concludes with a discussion of the numerous ties between this work and other efforts, and some final thoughts.

## 2. Algorithmic Details

Morphological operations form the basis of the standard approach for cleaning up noise after background subtraction and thresholding. In particular, the morphological techniques commonly applied consist of the two basic operations *dilation* and *erosion* applied in various combinations. Dilation expands the foreground of the image, adding a pixel to the foreground if any of its neighbors within a specified neighborhood of radius  $r$  (called the structuring element) are already part of the foreground. Erosion expands the background, removing a pixel from the foreground if any of its neighbors are background. These two operations may be combined; a dilation followed by an identical erosion is called a *closing*, and fills in holes in the foreground smaller than the neighborhood diameter. Likewise, an erosion followed by an identical dilation is called an *opening*, and may be used to eliminate isolated foreground pixels. Such operations are well studied, and more details may be found in reference texts [6].

Noise in the background-subtracted image tends to make some foreground pixels look like background, and vice versa. A morphological closing followed by an opening addresses these sources of error: the closing fills in the the missing foreground pixels (assuming that enough of their neighbors are correctly identified), and the opening removes extraneous foreground pixels surrounded by background. Care must be taken in choosing the radius for these operations. If the radius is too small, then larger clusters of noisy pixels will remain uncorrected; if too large, then legitimate detail in the foreground silhouette will be lost.

With particularly noisy background-subtracted images, mislabeled background pixels may become so numerous and closely spaced that the initial closing operation fills in

the gaps between them. Increasing the threshold  $\tau$  for the initial foreground-background segmentation prevents this undesirable effect by biasing the initial labeling away from the foreground. In other words, the higher threshold causes more foreground pixels to be classified as background than background pixels as foreground. Performing the initial closing operation corrects for this bias by closing the gaps between the correctly labeled foreground pixels.

### 2.1. Graph Cuts for Foreground Segmentation

Unlike the morphological approach, the graph-cut algorithm begins by building a graph based upon the image. Each pixel  $p_{ij}$  in the image generates a corresponding graph vertex  $v_{ij}$ . Two additional vertices form the source and sink, representing the foreground and the background respectively.

Figure 1 illustrates the graph formed for a small  $3 \times 3$  portion of the image plane. A typical vertex in the graph links to exactly six other nodes: the source and the sink, plus the the vertices of its four-connected neighbors. Vertices corresponding to pixels on the edge of the image will have fewer neighbor links, and the source and the sink will each connect to all the pixel vertices. The weights of the links between the pixel vertices and the source  $s$  and sink  $t$  derive directly from the difference between the current frame and the background at the corresponding pixel,  $\delta_{ij}$ :

$$w(s, p_{ij}) = \delta_{ij} \quad (1)$$

$$w(p_{ij}, t) = 2\tau - \delta_{ij} \quad (2)$$

The neighbor links (between pixel vertices) all have identical weights, equal to  $\tau$  times a second parameter  $\alpha$  (typically taking on values close to 1.0). The parameter  $\tau$  in the latter equation plays an analogous role to the threshold in the morphological algorithm, corresponding to the level above which the pixel associates more strongly with the foreground than the background.

The value of  $\alpha$  controls how strongly neighboring pixels tend to group. If  $\alpha$  is low, then neighboring pixels bond weakly and the end result will look much like that obtained by simply thresholding the output from the background subtraction. Conversely, high  $\alpha$  causes pixels to bond strongly with neighboring pixels, and the output will contain larger clusters of homogeneity. Noisy inputs thus tend to require larger values of  $\alpha$ , in order to smooth over the larger clusters of noisy pixels.

Once constructed, standard methods based upon graph flow will find an optimal (minimum cost) cut separating the source from the sink. Andrew Goldberg has kindly made optimized code for this computation available on the web [2]. Each node in the graph will lie on one side or the other of the optimal cut, remaining connected solely to the source

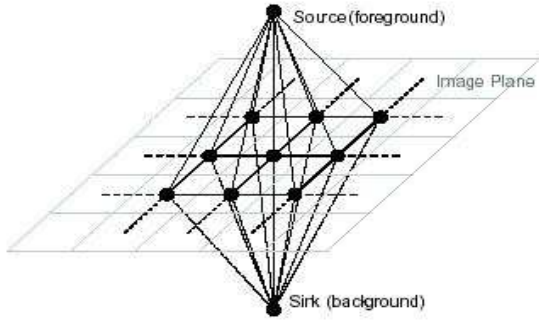


Figure 1: Graph construct embedded in image plane. Each pixel corresponds to a node, and all pixel nodes are connected to the source and the sink.

or to the sink. The algorithm labels those nodes still connected to the source as foreground, and those connected to the sink as background.

If desired, one may construct a graph to represent several frames of video at once. In this case, a typical pixel vertex connects to six neighbors (four spatial plus two temporal), but otherwise the construction remains the same. Using multiframe graphs can impose consistency of the result from one frame to the next, but trial experiments indicate no benefit in terms of overall accuracy. Therefore, the remainder of this paper focuses on single-frame graphs.

### 3. Synthetic Results

A preliminary set of experiments measures the performance of the two algorithms on artificial data. Using artificial data allows careful control of experimental conditions. Figure 2a shows the test pattern used, containing gradations in detail from coarse to fine. The right-hand portion of the image contains lines one pixel in width spaced a single pixel apart, and successive portions to the left double the width of both the lines and the gaps. Figures 2b and 2f show two images used as input to the algorithms, formed by taking the ground truth and adding noise. Noise at each pixel is sampled independently from a normal distribution of known variance, to generate an input with known signal-to-noise ratio (SNR). Figures 2c-2e and 2g-2i shows the results generated for the two inputs shown in 2b and 2f.

Table 1 gives the error rate on the best performance of each algorithm for a number of different SNR values, including those illustrated in Figure 2. As a baseline, it also gives the performance achieved by simply thresholding the input image. In addition to the error rates, the parameter values used to achieve the result also appear (except for  $\tau$  on the graph algorithm, which is always 0.5). The values given

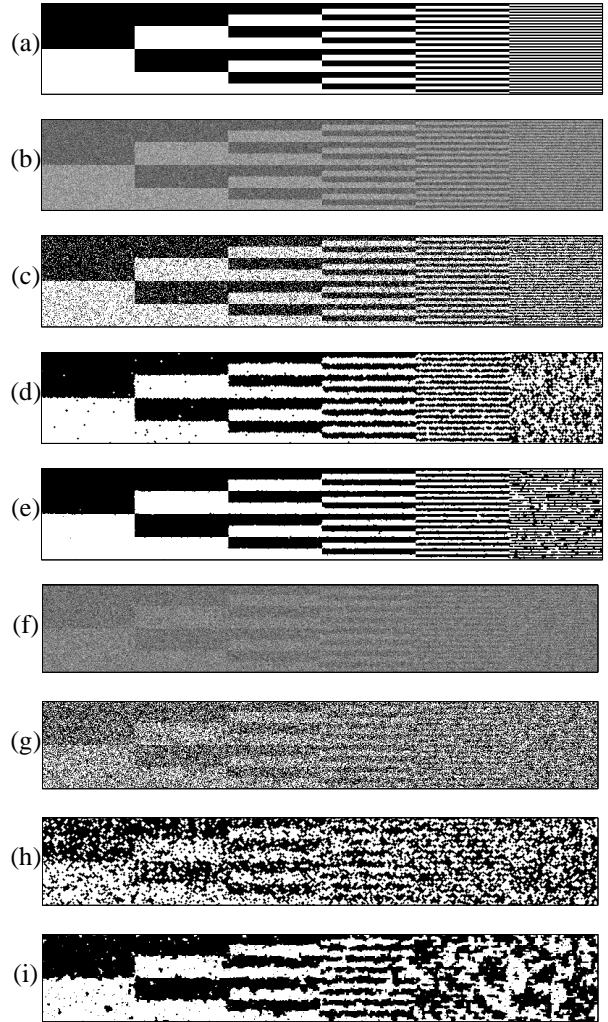


Figure 2: Segmentation results for synthetic data. (a) Ground truth; (b-e) SNR = 2.0 results: input signal, control (thresholded), morphological, graph; (f-i) SNR = 0.5 results: input signal, control (thresholded), morphological, graph.

Table 1: Error rates for the test patterns of Figure 2.

SNR	Thresh	Morph	$\tau$	$r$	Graph	$\alpha$
4	2.3%	2.3%	0.50	0	0.0%	0.8
2	15.8%	10.3%	0.70	1	2.8%	0.87
1.5	22.8%	13.5%	0.75	1	5.9%	0.95
1	30.9%	19.6%	0.95	1	11.2%	1.4
0.8	34.3%	23.8%	1.05	1	14.0%	1.8
0.65	37.3%	27.5%	1.20	1	16.7%	2.1
0.5	40.1%	31.4%	1.45	1	19.8%	2.5

correspond to the best result for a particular algorithm on a particular input.

The graph cut algorithm performs markedly better on the synthetic data than either the control or the morphological method at all signal-to-noise ratios. The error rate for the morphological techniques is always better than that for the control, except at the highest SNR (where they tie).

Examination of the graphical output in Figure 2 shows that at SNR = 2.0 both trial algorithms do fairly well, but the graph cut result displays cleaner edges and captures more of the fine detail at the highest resolution. The morphological result loses the details of the highest-resolution section at the right of the test image. At the SNR = 0.5, where the outlines of the input test pattern can barely be discerned by human eyes, the graph cut result still looks reasonable for the areas with coarser detail. Both algorithms lose the details in the two sections of highest resolution. Interestingly, increasing  $\alpha$  in the graph cut algorithm can further improve results on the low-resolution segments, albeit at the expense of further degradation at high and medium resolution.

## 4. Experiments With Real Images

The main set of experiments explores the performance of the algorithms on video taken under real world conditions. The three video clips used cover a range in quality and subject: from color clips shot both indoors and outdoors with fixed cameras, to a low-quality grayscale video of a ballet dancer with a panning camera and compression artifacts. The former represent relatively easy conditions, while the latter presents a stiffer challenge for background subtraction. Table 2 gives more details on each clip.

Each clip must undergo extensive preprocessing before reaching the stage where the algorithms on trial may be applied. Although some may object to the processing choices made here (particularly the use of static background models), changes in these choices would amount only to a change of the input to both trial algorithms, akin to choosing different videos for the tests. Neither of the approaches under consideration precludes algorithmic improvements to the preprocessing stages, but more complicated preprocess-

Table 2: Details on the video clips used for testing.

	Clip #2: Outdoor clip, regular motion, some reflection off glass. Fixed camera. 124 frames.
	Clip #1: Indoor clip with some shadowing, reflections off the floor. Some low contrast portions. Fixed camera. 160 frames.
	Clip #3: Grayscale MPEG video of a dancer. Low contrast. Panning camera. 99 frames.

ing introduces potentially confounding design decisions. Therefore, for simplicity and replicability, the experiments avoid sophisticated preprocessing where possible. For the first two clips, the experiments eschew the dynamically updated background models used by most current systems (e.g.,  $W^4$  [3]) in favor of a static background model computed over the entire clip. (A static background model is also comparable to a dynamic model that has been allowed to equilibrate.)

To prepare a video for background subtraction, a background model is built using crudely robust statistical techniques. The model builder takes the pixel color from every fourth frame, and throws out the data above and below a pair of thresholds (say the 25th and the 75th percentiles). From the remaining numbers it estimates the mean and variance of each pixel's color, assuming a normal distribution. This approach provides effective robustness to occlusions of the background on a small fraction of the video frames. (More complicated pixel modeling based upon mixtures of Gaussians can be used, but again this would only confound the comparison of the two algorithms under trial.)

For the third clip, the camera movement necessitates special treatment. Before building the background model described above, each frame must be registered with a canvas representing the entire background. A least-squares fit based on frame-to-frame optical flow generates an approximate set of initial registrations, expressed as affine transforms. The computer then builds up the canvas frame by frame, using function minimization to find the affine transform yielding the smallest disparities between the new frame and the median values on the existing canvas. The pixel values for the frame then get interpolated onto the can-



Figure 3: Registered median background model for Clip #3, *Dancer*. The camera pans from right to left, following the dancer.

vas, yielding new median values. Figure 3 shows the result of this process.

With the completed model (and registrations, if necessary) in hand, each frame can be compared with the mean background image. The difference at each pixel, normalized by the variance at that pixel, forms the raw data input to the two finishing algorithms. Typically the calculations might be carried out on each of the red, green, and blue (RGB) components of an image, and the differences in each component summed together. However, several modifications to the process provide necessary tolerance to shadows and lighting changes. Making the comparisons in the hue-saturation-value (HSV) color space causes disparities due to shadows to show up primarily in one channel, namely the pixel value ( $V$ ). Areas in shadow display lower  $V$  component values than the unshadowed background, but are similar in the other two components. Therefore, discounting small decreases (less than 5% of the total range) in  $V$  effectively ensures that shadowed background areas do not falsely appear to belong to the foreground. This method effectively mirrors other recent results [4], although that work differs superficially by processing images in RGB color space.

A suitable criterion must be chosen for grading the segmentation results. The total fraction of pixels in the image differing from ground truth appears an attractive error measure at first glance, but a closer look reveals flaws in this criterion. Figure 4d shows a segmentation created using morphological techniques with very large structuring element (a disk of radius 10). Although it captures few details of the subject figure's outline accurately, its error over the whole frame is 1.25%. Figure 4e and 4f show alternate segmentations that look more faithful to the exact outlines of the ground truth. Yet these have higher whole-frame errors of 2.24% and 2.59%, respectively, largely due to noise at the edges of the frame and other areas separate from the main figure.

In order to reward segmentations similar to Figure 4e and 4f, the experiments employ a modified error measure focus-

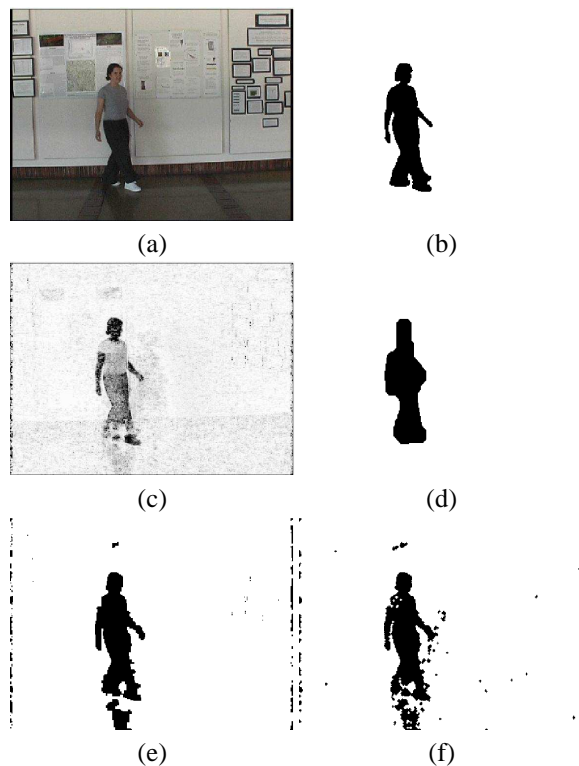


Figure 4: Effects of different error measurements. (a) Original image. (b) Ground truth. (c) Difference from background. (d) Best morphological segmentation by whole-image criterion. (e) Best graph and (f) morphological segmentations using the connected components criterion.

ing specifically on the moving figure in the clip. The measure first computes the connected components of the segmented foreground and identifies all the components that overlap with ground truth (as identified by a human operator tracing the figure's outline in Photoshop). Pixels in the selected components that do not overlap with ground truth count as false positives, while ground truth areas identified as background by the segmentation algorithm count as false negatives. Combining the number of false positives and false negatives, then scaling by the number of pixels in the ground truth yields the error measurement for the frame.

#### 4.1. Real Image Results

Table 3 shows the error rates of both the morphological and graph algorithms on the video inputs, after tuning the algorithm parameters for best results. (Interestingly, although larger structuring elements were tested for the morphological operations, small radius-one disk-shaped elements give the best results on all three clips.) Examining the numbers, one sees that the quality of the video input forms the largest factor determining the error, with far more mistakes for ei-

Table 3: Summary of foreground segmentation results (connected components error criterion).

Clip	Morph	Graph
1. Outdoor	0.164	0.161
<i>Params:</i>	$\tau = 20.3, r = 2$	$\tau = 16.2, \alpha = 0.94$
2. Indoor	0.154	0.133
<i>Params:</i>	$\tau = 5.21, r = 1$	$\tau = 4.87, \alpha = 0.81$
3. Dancer	0.541	0.532
<i>Params:</i>	$\tau = 2.26, r = 1$	$\tau = 2.15, \alpha = 0.97$

ther approach on the *Dancer* clip. Nevertheless, the graph-based algorithm performs significantly better (in a statistical sense) on every clip tested, according to a paired sample t-test.

Although the numeric differences appear small, their psychological importance can be large, with the numbers unable to tell the entire story. The presence or absence of a body part such as a forearm may alter the error by as little as 0.04 or so, while a one-pixel shift distributed evenly around the entire the segmentation boundary can alter the error by 0.12 or more. To illustrate what the error values cannot, Figures 5–7 show sequences of frames from each clip, spread evenly across time. (Frames where the subject is entering or exiting the screen are not shown.)

Compared side by side, the graph based result (right column) typically appears “cleaner” than the morphological result, and adheres more faithfully to the contours of the ground truth. The *Indoor* clip best displays the advantages of the graph algorithm, showing a smoother boundary and less frequent inclusion of background. Although the graph algorithm does better on all three clips, *Outdoor* is mostly too easy to show up the differences, and *Dancer* is too hard. The errors evident in the *Dancer* clip demonstrate that any contrast-based algorithm will fail where the input is deceptive (due to low contrast between foreground and background, heavy shadowing, reflections, noise, etc.). High quality input remains crucial, regardless of the algorithm applied.

## 5. Related Work and Conclusions

Graph cuts can produce a cleaner foreground segmentation based upon frame-by-frame comparisons with a background model. This result may not surprise those who have been following the use of graph-based methods for other applications. This paper combines advances from several different research threads that have not previously been applied to the specific problem of foreground segmentation. Given the status of foreground segmentation as the precursor to a host of other applications, any advance which can improve the segmentation quality may have wide-ranging

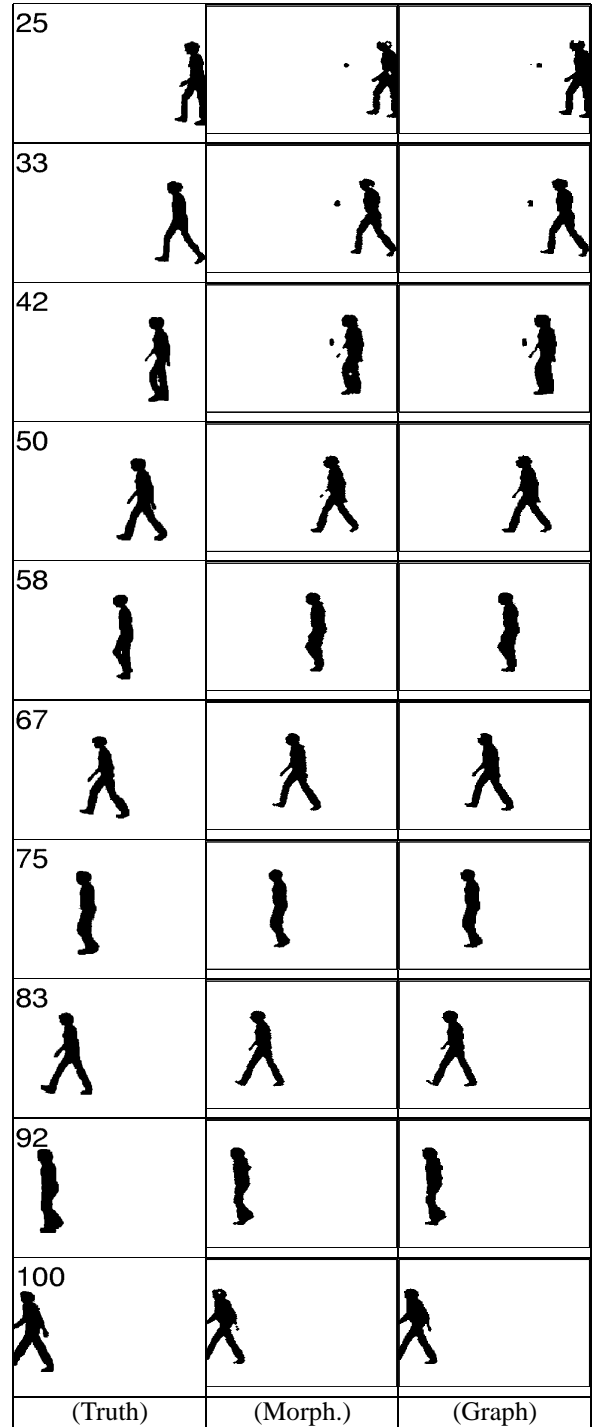


Figure 5: A sequence of frames from the *Outdoor* clip. The extra spot in earlier time frames is a reflection.

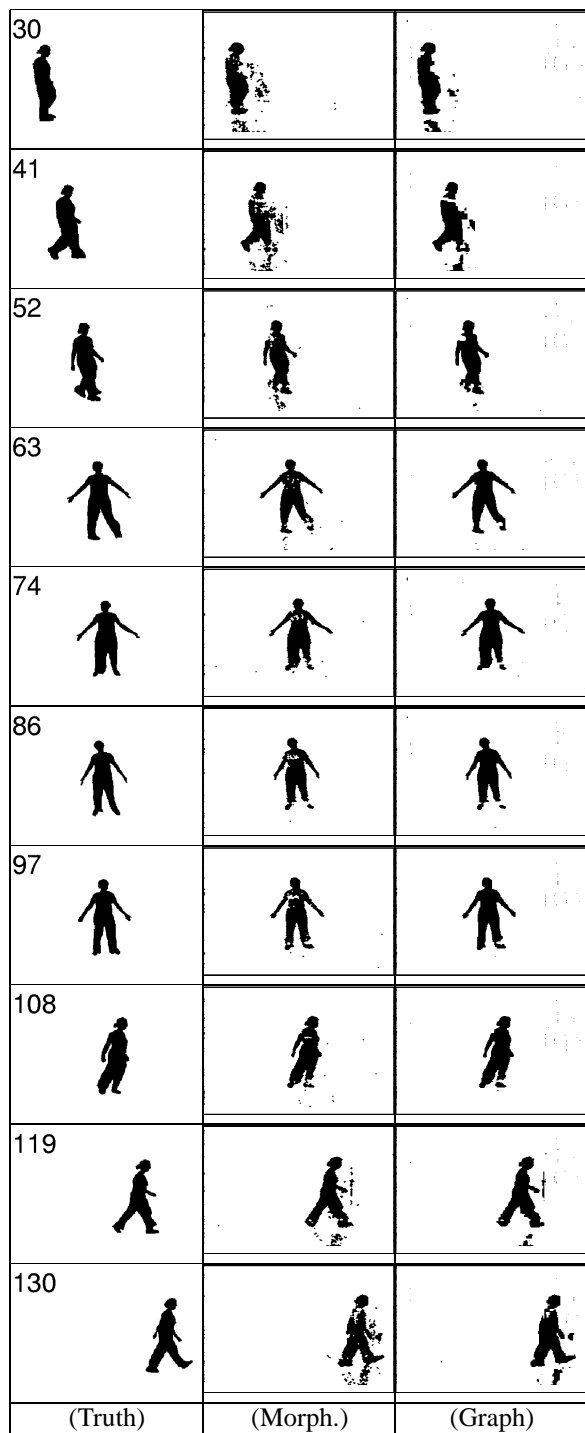


Figure 6: A sequence of frames from the *Indoor* clip. The subject's shirt provides low contrast with the background.

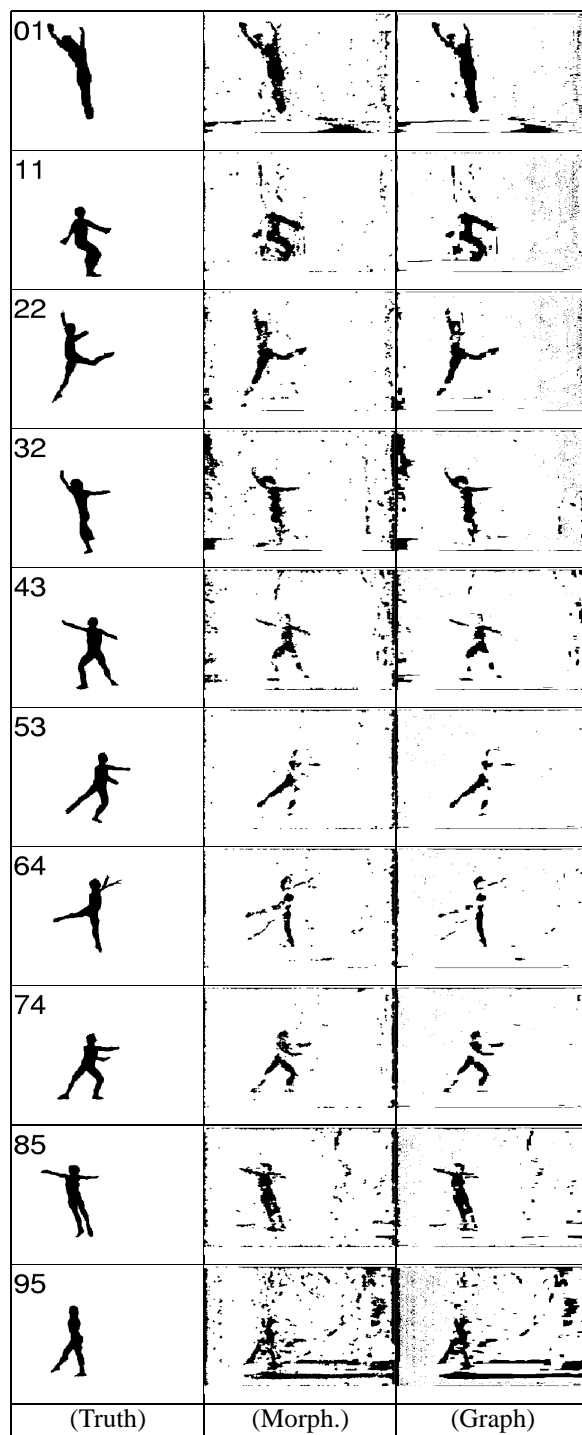


Figure 7: A sequence of frames from the *Dancer* clip. The dancer's costume blends with the background in many places.

effects. The experimental results show that the borrowed techniques produce excellent results, as they have in other fields.

## 5.1. Previous Work

Although the use of a 2-way cut for foreground segmentation is novel, other kinds of graph-based methods have received considerable attention recently for segmentation applications. In particular, methods based upon the *minimum normalized cut* (n-cut) have achieved notable success in general segmentation problems [8]. General segmentation (with the goal of subdividing any image into coherent regions without *a priori* knowledge of its contents) is a much more difficult problem than foreground segmentation with a static background, as explored herein. Not surprisingly therefore, n-cut algorithms for general segmentation differ from this paper's approach, typically employing a fully-connected graph requiring approximation methods to solve [7]. By contrast, the algorithm described herein uses a graph that represents only local connections among pixels. Because the number of links remains linear in the number of nodes, this local-only graph can be solved easily and exactly. Furthermore, the advantages of the normalized cut over the standard cut do not apply in the local-only case, because the energy of a cut relates only indirectly to the number of nodes on either side.

A more direct connection to the current work may be drawn from research on image correspondance for stereo vision and visual correspondance [1, 9]. Again, the stereopsis problem is more difficult than foreground segmentation, requiring a selection among multiple hypothesized displacements at each pixel. The work mentioned above therefore employs algorithms to approximate a multiway cut on a graph representing the image. The algorithm herein embodies a special case of such a situation, where the existence of only two categories to distinguish (foreground and background) allows the use of an exact 2-way cut solution.

In the processing of the video frames prior to the thresholding step, this work follows current the state of the art. In particular, it builds probability models for the distribution of measured color values at each pixel [5]. It further employs techniques to eliminate interference from shadows; similar measures were recently described elsewhere [4]. The authors of the latter work note that their segmentation process runs in real time, which is a challenge for the new algorithm due to the graph cut step. Theoretical bounds on this step are  $O(n^2 \log n)$ , although for some problem classes the actual performance can be quadratic or better [2]. Empirically, it appears that real time processing is still possible at lowered resolution, and this stricture should ease with time as processor speeds increase.

## 5.2. Final Thoughts

Using graph cuts for foreground segmentation produces cleaner and more accurate results than the currently prevailing approach based upon morphological operations. The graph-based technique appears better at overcoming the effects of noise by aggregating information from a local neighborhood around each pixel, while remaining true to the underlying data. On test using synthetic data, it cut the error rate by at least a third over the current methods for the noisiest input, and by a greater factor for the less noisy cases. On real data, the method significantly reduces error over current methods, although it cannot magically cure problems associated with low quality input data. The one disadvantage of the graph-based method is its speed; empirically it runs more slowly or at lower resolution than the morphological operations.

Given the range of applications that use background subtraction, adoption of the new technique seems likely to provide significant benefits in a number of areas. In addition to current uses for background subtraction, the higher fidelity of the graph-cut method may open up new applications not hitherto feasible because they require highly reliable input. In any case, graph cuts for foreground segmentation deserve a place in the research scientist's bag of tools.

## References

- [1] Y. Boykov, O. Veksler, and R. Zabih. Efficient approximate energy minimization via graph cuts. *IEEE Transactions on Pattern Analysis and Machine Intelligence*, 20(12):1222–1239, November 2001.
- [2] B. V. Cherkassky and A. V. Goldberg. On implementing the push-relabel method for the maximum flow problem. *Algorithmica*, 19(4):390–410, 1997.
- [3] I. Haritaoglu, D. Harwood, and L. S. Davis.  $W^4$ : Real-time surveillance of people and their activities. *IEEE Transactions on Pattern Analysis and Machine Intelligence*, 22(8):809–830, August 2000.
- [4] T. Horprasert, D. Harwood, and L.S. Davis. A robust background subtraction and shadow detection. In *Proceedings of the Asian Conference on Computer Vision*, 2000.
- [5] K.-P. Karmann and A. von Brandt. Moving object recognition using an adaptive background memory. In *Time-Varying Image Processing and Moving Object Recognition*, Amsterdam, 1990. Elsevier.
- [6] *Image Processing Toolbox*, chapter 9: Morphological Operations. The Mathworks, 2001.
- [7] J. Shi, S. Belongie, T. Leung, and J. Malik. Image and video segmentation: The normalized cut framework. In *Proceedings of the IEEE Conference on Image Processing*, pages 943–947, Oct 1998.

- [8] J. Shi and J. Malik. Normalized cuts and image segmentation. *IEEE Transactions on Pattern Analysis and Machine Intelligence*, 22(8):888–905, 2000.
- [9] O. Veksler. Stereo matching by compact windows via minimum ratio cycle. In *International Conference on Computer Vision*, pages 540–547, July 2001.

130

